Microsystem Technologies 10 (2004) 338–344 © Springer-Verlag 2004
DOI 10.1007/s00542-004-0380-9

# Effects of thrust hydrodynamic bearing stiffness and damping on disk-spindle axial vibration in hard disk drives

**T. Jintanawan, C.-P. Roger Ku, J. Zhu**



**Abstract** This paper aims at investigating the effects of variations in thrust hydrodynamic bearing (HDB) parameters such as axial stiffness and damping coefficients on the axial vibration of disk-spindle systems in hard disk drives. For a parametric study, a closed-form axial frequency response function (FRF) of HDB spindle systems is derived as a function of the axial stiffness and damping coefficients of thrust HDBs. It is known that the axial vibration of the disk-spindle system is composed of two main parts: the vibration of the rigid hub in the axial direction and the disk deflection in the transverse direction. The results from this research clearly show that the vibration amplitudes at low frequency range is dominated by the axial vibration of the hub, and the amplitude of the unbalanced (0,0) mode is dominated by the disk deflection. The parametric study reveals that at low frequency range an increase in the bearing stiffness significantly reduces the hub axial vibration, and hence the axial vibration of the disk-spindle system. Surprisingly, a too much increase in the damping results in a higher amplitude of the unbalanced (0,0) mode. This is because a heavy damping constrains the hub vibration to nearly no motion, resulting in a direct transmission of vibration from the base to disk. To confirm the parametric study, a vibration test was performed on two HDB spindle motors with identical design but different fluid viscosity. The higher viscosity represents the higher axial stiffness and damping in the thrust bearing. The test result indicates that the spindle motor with higher viscosity has a larger unbalanced (0,0) mode amplitude when subjected to an axial base excitation.

## 1 Introduction

Currently, hydrodynamic bearing (HDB) spindle motors are widely used in hard disk drives (HDDs) because of their capabilities for vibration suppression and acoustic noise reduction. Design criteria for the HDB spindles are reliability, low power consumption, and low vibration and shock responses (Asada et al. 2001; Matsuoka et al. 2001). As the spin speed and the density of HDD increase, the design of both radial and thrust bearings are a key to minimize the vibration of the HDB spindles. The radial HDBs are designed to suppress the rocking vibration which is the major contribution to track misregistration (Jintanawan 2002). The thrust HDBs have an impact not only on the rocking vibration but also on the axial vibration. The thrust HDBs provide rocking restoring and damping moments as well as axial restoring and damping forces. However only the axial forces have a great effect on the axial vibration. Suppression of this axial vibration through optimization of the thrust HDB parameters would be a practical and inexpensive solution. Experimental study on the effect of the thrust HDBs on the axial vibration of the disk-spindle systems for HDD was conducted by Ku (1997). In his study, the disk-spindle systems with four types of thrust HDBs, representing different compliance or stiffness, were tested. He has concluded that the compliance of the thrust HDB characterizes the axial vibration at low frequency range whereas the disk flexibility and/or disk clamping condition characterizes the disk (0,0) modes. However how the damping of the thrust HDBs affects the axial vibration of the disk-spindle systems for HDD is still open thus far.

This paper aims at investigating the effects of variations in the thrust HDB parameters, such as the axial stiffness and damping coefficients, on the axial vibration of the disk-spindle systems under an axial base excitation. For the parametric study, the mathematical model developed by Shen (1997) is modified to predict the axial frequency response functions (FRFs) of the HDB spindle systems for each set of the thrust HDB parameters. A closed-form FRF measured along the axial direction is then derived as a function of the axial stiffness and damping coefficients. Finally, two HDB spindle motors with different fluid viscosity are tested to support the findings.

## 2 Mathematical model

In this section, the equations of motion governing the *axial* vibration of HDB spindle systems are described. The equations of motion for HDB spindles are derived using Lagrange's method. The detailed derivation of these equations of motion is presented in Jintanawan et al. (1999) and Jintanawan et al. (2001). Figure 1 shows a physical model of disk-spindle systems with HDBs. The

*Received: 6 October 2003 / Accepted: 16 December 2003*

T. Jintanawan
Department of Mechanical Engineering,
Chulalongkorn University,
Bangkok, Thailand 10330

C.-P. Roger Ku, J. Zhu (✉)
Western Digital Corporation,
San Jose, CA 95138, USA
e-mail: Jiasheng.zhu@wdc.com

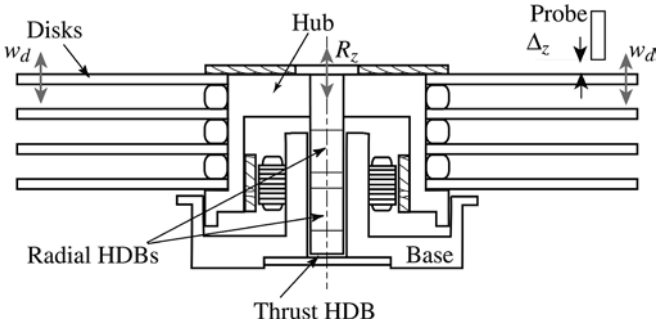


**Fig. 1.** A disk-spindle model with HDBs

system consists of $N$ elastic circular disks clamped to a deformable hub that allows infinitesimal rigid-body translation and rocking. The hub is press-fit onto a rotating, flexible shaft which is mounted to the base through two radial HDBs and a double-sided thrust HDB. The fluid bearings are modeled as generalized internal forces through in-line and cross stiffness and damping coefficients. In this model, the spindle system is axisymmetric and all the disks are identical. Because of the insignificance of the disk vibration modes with one or more nodal circles, only the zero-nodal-circle modes are retained in the mathematical model. Moreover the motion of the hub in the transverse and axial directions are completely decoupled. The spindle system is subjected to an axial base excitation and thus exhibits only the axial vibration.

From Jintanawan et al. (1999) and Jintanawan et al. (2001), vibration of the spindle systems is categorized into three sets of coupled motion: (a) coupled hub transverse translation-rocking, shaft deflection, and one nodal diametral disk modes; (b) coupled axial hub translation and axisymmetric disk modes; and (c) vibration mode of each disk with two or more nodal diameters. In this paper, we will focus only on the coupled axial motion (b). This axial motion is described by the following two groups of degrees of freedom: infinitesimal rigid-body translation $R_z$ of the spindle centroid in the axial direction, and axisymmetric eigenmodes of each disk $q_{00}^{(i)}$ $(i = 1, 2, \ldots, N)$, where the first and second indices *zeros* refer to the axisymmetric disk modes with zero nodal circle and zero nodal diameter. The equation of motion governing the axial hub translation and axisymmetric disk modes is

$$\mathbf{M}\ddot{\mathbf{q}}(t) + \mathbf{C}\dot{\mathbf{q}}(t) + \mathbf{K}\mathbf{q}(t) = \mathbf{f}(t) \tag{1}$$

where $\mathbf{q}$ is a vector of the generalized coordinates, $\mathbf{M}$ is the inertia matrix, $\mathbf{C}$ is the damping matrix, and $\mathbf{K}$ is the stiffness matrix given by

$$\mathbf{q} = \left(R_z, q_{00}^{(1)}, q_{00}^{(2)}, \cdots, q_{00}^{(N)}\right)^{\mathrm{T}} \tag{2}$$

$$\mathbf{M} = \begin{bmatrix} \eta & b_0 & b_0 & \cdots & b_0 \\ b_0 & 1 & 0 & \cdots & 0 \\ b_0 & 0 & 1 & \cdots & 0 \\ \vdots & \vdots & \vdots & \ddots & \vdots \\ b_0 & 0 & 0 & \cdots & 1 \end{bmatrix} \tag{3}$$

$$\mathbf{C} = \mathrm{diag}[c_z, \zeta, \zeta, \cdots, \zeta] \tag{4}$$

$$\mathbf{K} = \mathrm{diag}[k_z, \omega_{00}^2, \omega_{00}^2, \cdots, \omega_{00}^2] \tag{5}$$

$\mathbf{f}(t)$ is a vector of the generalized forces associated with the vertical base acceleration $\ddot{s}_z(t)$ given by

$$\mathbf{f} = -\ddot{s}_z(t)\begin{pmatrix} \eta \\ b_0 \\ \vdots \\ b_0 \end{pmatrix} \tag{6}$$

Detailed description of each term in $\mathbf{M}$, $\mathbf{C}$, $\mathbf{K}$, and $\mathbf{f}(t)$ is given in the Appendix.



## 3 Frequency response function (FRF)

In this section, a closed-form frequency response of the axial vibration $\Delta_z(t)$ is derived as a function of the total axial stiffness and damping coefficients $k_z$, and $c_z$. The amplitude of this frequency response will be used for the parametric study of the thrust HDBs in Sect. 4.

Consider the disk-spindle systems subjected to a harmonic base acceleration $\ddot{s}(t) \equiv \cos\omega t$. From (6), the generalized force of this harmonic base acceleration can be written as

$$\mathbf{f} = -\begin{pmatrix} \eta \\ b_0 \\ \vdots \\ b_0 \end{pmatrix}\cos\omega t \tag{7}$$

From (1), the steady-state response $\mathbf{q}(t)$ when subjected to the harmonic base acceleration is

$$\begin{aligned}\mathbf{q}(t) &= -\frac{1}{2}\left[\mathbf{H}(j\omega)e^{j\omega t} + \mathbf{H}(-j\omega)e^{-j\omega t}\right][\eta,\ b_0, \cdots, b_0]^{\mathrm{T}} \\ &\equiv \frac{1}{2}\left[\bar{\mathbf{Q}}(j\omega)e^{j\omega t} + \bar{\mathbf{Q}}(-j\omega)e^{-j\omega t}\right]\end{aligned} \tag{8}$$

where $\mathbf{H}(j\omega)$ is the complex frequency response function matrix given by

$$\mathbf{H}(j\omega) = \left[-\omega^2\mathbf{M} + j\omega\mathbf{C} + \mathbf{K}\right]^{-1} \tag{9}$$

By expanding the terms in the bracket on the right-hand side of (9), $\mathbf{H}(j\omega)$ can be written as

$$\mathbf{H}(j\omega) = \begin{bmatrix} A & B & B & \cdots & B \\ B & C & 0 & \cdots & 0 \\ B & 0 & C & \cdots & 0 \\ \vdots & \vdots & \vdots & \ddots & \vdots \\ B & 0 & 0 & \cdots & C \end{bmatrix}^{-1} \tag{10}$$

where

$$A = \left(k_z - \eta\omega^2\right) + jc_z\omega \tag{11}$$

$$B = -b_0\omega^2 \tag{12}$$

$$C = \left(\omega_{00}^2 - \omega^2\right) + j\zeta\omega \tag{13}$$

Due to the particular form of (10), $\mathbf{H}(j\omega)$ can then be rewritten using the matrix inversion (Shen 1997) as

$$\mathbf{H}(j\omega) = \frac{\mathbf{p}\mathbf{p}^{\mathrm{T}}}{FC} + \frac{1}{C}\mathrm{diag}[\,0 \quad 1 \quad \cdots \quad 1\,] \tag{14}$$

where

$$F = AC - NB^2 \tag{15}$$

$$\mathbf{p} = (\, C, \quad -B, \ \cdots, \ -B \,)^{\mathrm{T}} \tag{16}$$

Note that the notation $\bar{\mathbf{Q}}(j\omega)$ introduced in (8) is the frequency response vector with respect to a unit complex base acceleration $\ddot{s}(t) = e^{j\omega t}$. $\bar{\mathbf{Q}}(j\omega)$ is related to $\mathbf{H}(j\omega)$ as follows



$$\bar{\mathbf{Q}}(j\omega) \equiv \begin{pmatrix} \bar{R}_z(j\omega) \\ \bar{q}_{00}^{(1)}(j\omega) \\ \vdots \\ \bar{q}_{00}^{(N)}(j\omega) \end{pmatrix} = -\mathbf{H}(j\omega)[\,\eta, \quad b_0, \ \cdots, \ b_0\,]^{\mathrm{T}} \tag{17}$$

For the parametric study, the frequency response vector $\bar{\mathbf{Q}}(j\omega)$ needs to be derived in terms of the bearing parameters $k_z$ and $c_z$. By substituting (14) into (17) and then expanding (17), $\bar{\mathbf{Q}}(j\omega)$ can be derived as

$$\bar{\mathbf{Q}}(j\omega) \equiv \begin{pmatrix} \bar{R}_z(j\omega) \\ \bar{q}_{00}^{(1)}(j\omega) \\ \vdots \\ \bar{q}_{00}^{(N)}(j\omega) \end{pmatrix} = \frac{1}{F} \begin{pmatrix} \eta\left[(\omega_{00}^2 - \omega^2) + j\zeta\omega\right] + Nb_0^2\omega^2 \\ b_0(k_z + jc_z\omega) \\ \vdots \\ b_0(k_z + jc_z\omega) \end{pmatrix} \tag{18}$$

It is observed from (18) that each component in $\bar{\mathbf{Q}}(j\omega)$ is a complex value containing the information of the response amplitude and the phase.

In practice the axial response $\Delta_z(t)$ of the spindle systems can be measured at an arbitrary point (with radius $r$) on the top disk from the ground-based observer as shown in Fig. 1. The measured response $\Delta_z(t)$ consists of two components of motion: the axial hub translation $R_z(t)$, and the axisymmetric vibration of the disk $w_d(r, t)$. $\Delta_z(t)$ is given by

$$\Delta_z(t) = R_z(t) + w_d(r, t) \tag{19}$$

where $w_d(r, t)$ is discretized through the following approximation function

$$w_d(r, t) = R_{00}(r) q_{00}^{(N)}(t) \tag{20}$$

where $R_{00}(r)$ and $q_{00}^{(N)}(t)$ are the axisymmetric shapefunction and the $N$-th eigenmode, respectively. $\Delta_z(t)$ is calculated by first solving (1) for $R_z(t)$ and $q_{00}^{(N)}(t)$, and then substituting (20) into (19).

From (19) and (20), the measured axial frequency response $\bar{\Delta}_z(j\omega)$ when subjected to a unit harmonic base acceleration is obtained as

$$\bar{\Delta}_z(j\omega) = \bar{R}_z(j\omega) + R_{00}(r)\bar{q}_{00}^{(N)}(j\omega) \tag{21}$$

Substituting (18) into (21) yields

$$\bar{\Delta}_z(j\omega) = \frac{P + jQ}{F} \tag{22}$$

where

$$P = b_0 k_z R_{00}(r_0) + \eta\omega_{00}^2 + (Nb_0^2 - \eta)\omega^2 \tag{23}$$

**Table 1.** Geometry and Properties of a four-disk spindle system supported by HDBs

| Disk-spindle system | |
|---|---|
| $b$ | 47.50 mm |
| $a$ | 15.24 mm |
| $I_1$ | 8.56 kg mm$^2$ |
| $M$ | $7.87 \times 10^{-2}$ kg |

and

$$Q = [b_0 c_z R_{00}(r_0) + \eta_0\zeta]\omega \tag{24}$$

The amplitude of $\bar{\Delta}_z(j\omega)$ is

$$\left|\bar{\Delta}_z(\omega, k_z, c_z)\right| = \left[\frac{P^2 + Q^2}{|F_0|^2}\right]^{\frac{1}{2}} \tag{25}$$

## 4 Parametric study of thrust HDBs

In this section, the effects of variations in thrust HDB parameters such as the axial stiffness and damping coefficients on the axial FRF are investigated through the numerical simulation. The disk-spindle system under consideration consists of four identical disks with a thickness of 0.8 mm. The spindle spins at 7200 rpm. The disk-spindle parameters excepted the bearing coefficients are described in Table 1. The axial stiffness and damping parameters of the thrust HDB are inherently dependent; i.e., design of thrust HDB to increase the stiffness will increase the damping and vice versa. Both stiffness and damping parameters can be changed through changes in the bearing geometries and axial-gap height, the fluid viscosity, and etc. (Jang and Kim 1999). In this paper, five sets of the axial stiffness and damping coefficients of the thrust HDBs, collected from various bearing designs, were used for the parametric study and the optimization. The values of stiffness and damping coefficients for these five data sets are summarized in Table 2 and plotted in Fig. 2.

Figure 3 shows the axial FRF of the disk-spindle system obtained from (25) when the radius $r$ of measurement is 0.042 m, and both the axial stiffness and damping coefficients are varied according to Table 2. The resonance peak around 600 Hz for each bearing design is the unbalanced (0,0) mode. For this mode, all disks exhibit in-phase axisymmetric vibration and the hub undergoes axial vibration (Shen 1997). The shape of this unbalanced (0,0) mode is shown in Fig. 4. As seen in Fig. 3, with an increase in both stiffness and damping (the stiffness and damping

**Table 2.** Axial stiffness and damping coefficients of five different thrust bearing designs

| Data set | $\sum_t k_{zz}^{(t)}$ (N/m) | $\sum_t c_{zz}^{(t)}$ (Ns/m) |
|---|---|---|
| 1 | $4.974 \times 10^4$ | $1.581 \times 10^2$ |
| 2 | $2.368 \times 10^5$ | $4.958 \times 10^2$ |
| 3 | $5.584 \times 10^5$ | $1.013 \times 10^3$ |
| 4 | $1.108 \times 10^6$ | $2.130 \times 10^3$ |
| 5 | $1.690 \times 10^6$ | $3.247 \times 10^3$ |

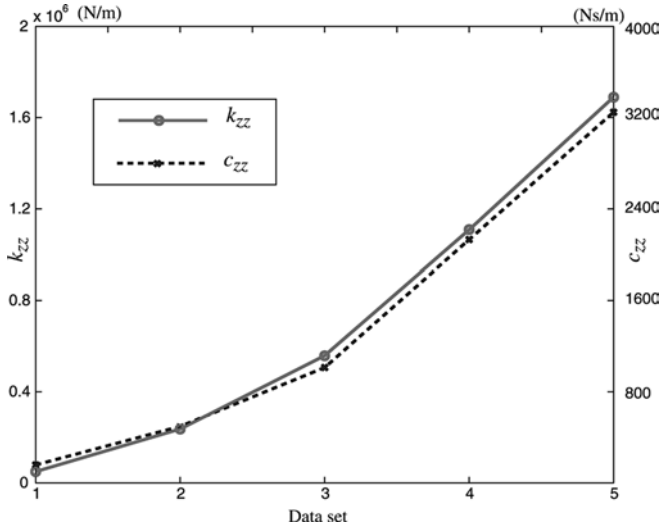


**Fig. 2.** $k_{zz}$ and $c_{zz}$ for five different thrust bearing designs

coefficients change from bearing design 1 to 5 in Table 2), the vibration amplitude at low frequency range (<400 Hz) is reduced. However, higher axial stiffness and damping result in higher amplitude of the unbalanced (0,0) mode.

Figures 5 and 6 show the FRFs of axial vibration components: the axial hub translation $|\bar{R}_z|$ and the disk deflection $|\bar{w}_d|$ at radius $r$ of 0.042 m, when both the stiffness and damping coefficients are varied. Compared with the total axial vibration in Fig. 3, it can be seen from Figs. 5 and 6 that the large amplitude of the axial vibration at low frequency range (<400 Hz) is dominated by the axial hub vibration while the unbalanced (0,0) mode is dominated by the disk deflection.

To investigate the effect of variation in only the axial stiffness or only the axial damping on the axial vibration, the numerical simulation was performed by varying each parameter at a time. Figures 7 and 8 show the axial FRF of the disk-spindle system when varying only the axial

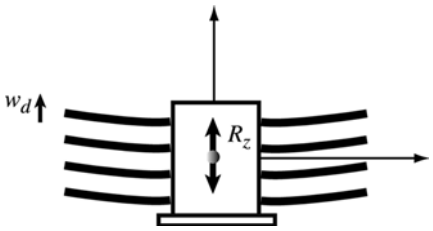


**Fig. 4.** Shape of the unbalanced (0,0) mode



stiffness and only the axial damping, respectively. As seen in Fig. 7, an increase in the axial stiffness suppresses the axial vibration at low frequency range (<400 Hz). Specifically, larger stiffness significantly reduces the axial hub vibration which is the major component of the axial vibration in the low frequency range. Moreover with the larger stiffness, the amplitude of the unbalanced (0,0) mode around 600 Hz slightly increases as shown in Fig. 7. Let's now consider the damping effect in Fig. 8. An increase in the axial damping decreases the amplitude at the low frequency range, but surprisingly increases the amplitude of the unbalanced (0,0) mode. At resonance, the larger damping slightly reduces the axial hub vibration but significantly increases the disk deflection which is the major component in the unbalanced (0,0) mode. From Figs. 7 and 8, an increase in either axial stiffness or axial damping causes a higher amplitude of the unbalanced (0,0) mode. However the axial damping has a greater effect on the amplitude of this mode.

For a clear explanation of damping effect on the unbalanced (0,0) mode, a model of HDB spindle with single disk is considered. This model is equivalent to a two-degree-of-freedom discrete system in Fig. 9, where $m_1$ and $m_2$ represent the masses of the hub and the disk, respectively. In addition, $k_1$ and $c_1$ are the axial stiffness and damping coefficients of the thrust HDB, whereas $k_2$ and $c_2$ are the equivalent disk stiffness and damping. $x_1$ and $x_2$ in Fig. 9 represent the axial hub vibration and

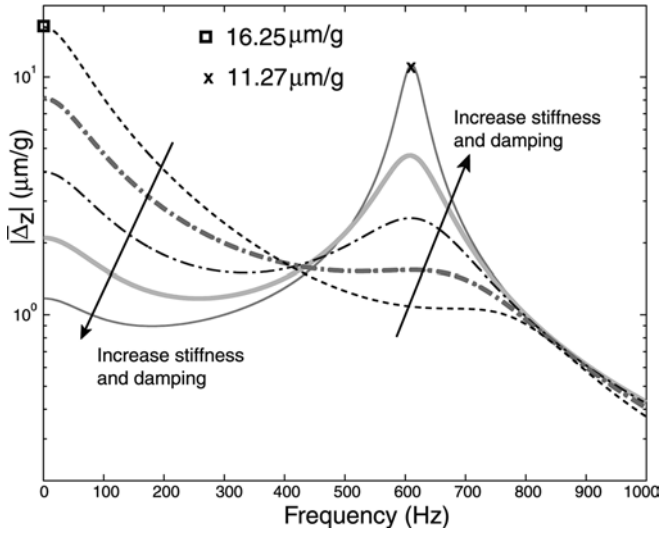


**Fig. 3.** Axial FRF of the disk-spindle system when the axial stiffness and damping coefficients are varied

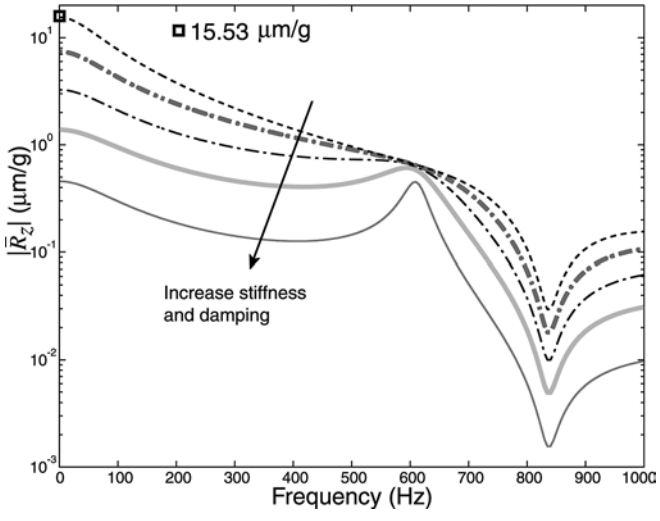


**Fig. 5.** FRF of the hub axial translation when the axial stiffness and damping coefficients are varied

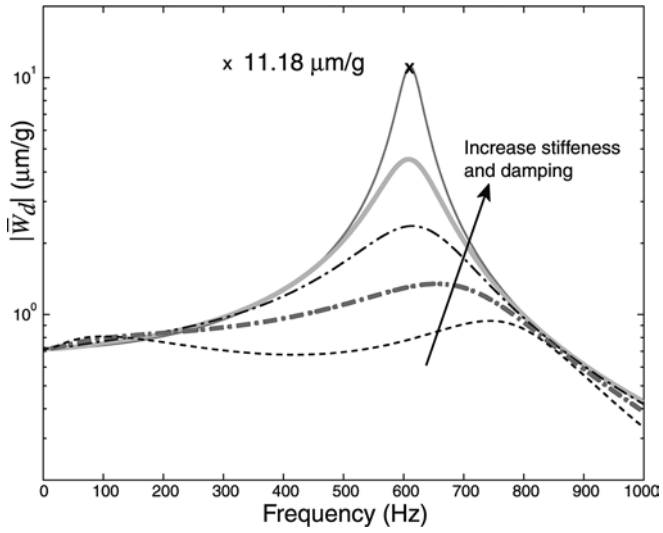


**Fig. 6.** FRF of the disk deflection when the axial stiffness and damping coefficients are varied

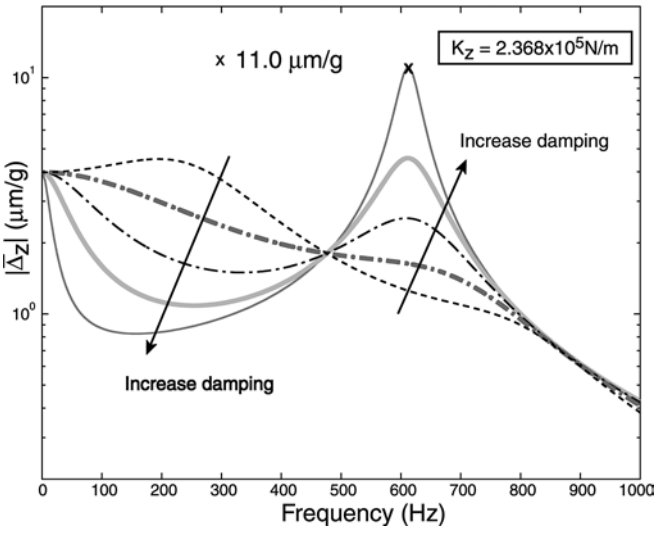


**Fig. 8.** Axial FRF of the disk-spindle system when only the axial damping coefficient is varied

the total axial vibration measured at the outer rim of the disk, respectively. In this stated problem, the damping coefficient $c_1$ is tuned to reduce the axial vibration $x_2$.

Figure 10 shows the FRF of the axial vibration $x_2$ subjected to the base excitation $\ddot{s}_z(t)$ when the damping $c_1$ is varied. With a light damping ($c_1$ < 100 Ns/m), there exist two resonance modes at the frequency around 450 and 1100 Hz. This is natural because the system has two degrees of freedom. Moreover an increase of damping from 10 to 100 Ns/m reduces both resonance amplitudes. However as the damping becomes larger (>100 Ns/m), a new lightly damped resonance develops at 900 Hz. This is probably because a very large damping powerfully suppresses the vibration $x_1$ so that there is nearly no motion (pin-support like) for $m_1$. Hence the system behaves similar to a one-degree-of-freedom system, having its own single resonance. With a high constraint at mass $m_1$, the excitation tends to transmit directly from the base to mass $m_2$. Thus a too much increase in the damping $c_1$ leads to an undesirable large vibration of $x_2$ at the new resonance. This phenomena would occur to the HDB spindle with more than one disks. In conclusion, a too much increase in the axial damping of the thrust bearing most likely constrains the hub motion, allowing the vibration to be transmitted from the base to the disks directly. Therefore the larger value of damping results in a higher amplitude of the unbalanced (0,0) modes.

The parametric study is useful for the design of thrust HDBs. In practice, an optimal value of the axial damping in the thrust HDBs can be desired to minimize the amplitude of the unbalanced (0,0) mode. With the optimal axial damping, the corresponding axial stiffness does not minimize the axial vibration at low frequency range. This undesirable axial vibration at low frequency range, however, can be compensated by the servo system in HDD.

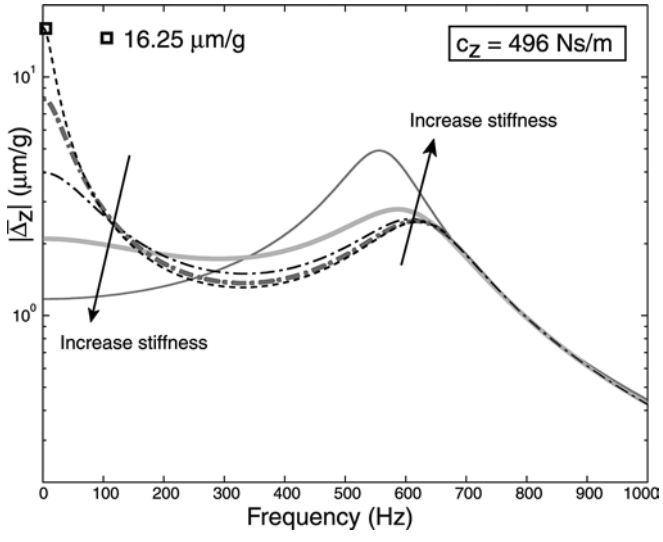


**Fig. 7.** Axial FRF of the disk-spindle system when only the axial stiffness coefficient is varied

## 5 Experimental test

To confirm the study of the axial stiffness and damping effect, a vibration test was performed on two identical HDB spindles with different fluid viscosity. The fluid viscosities of these two spindles are listed in Table 3. Both

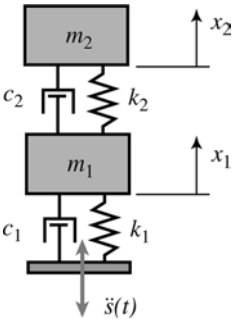


**Fig. 9.** A two-degree-of-freedom discrete model

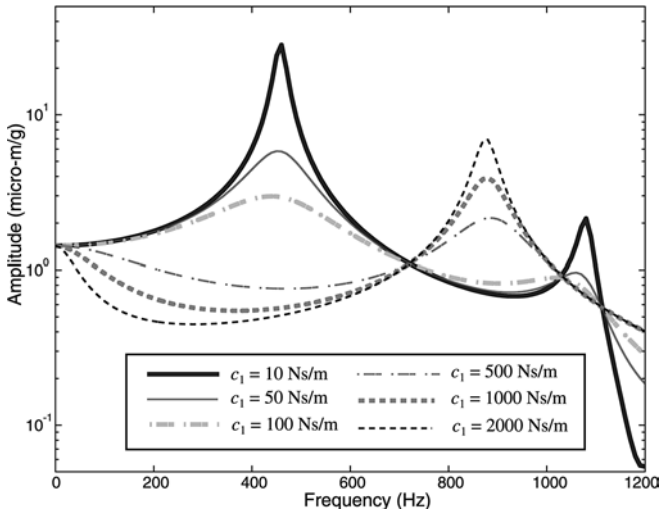


**Fig. 10.** Effect of damping on vibration of a two-degree-of-freedom discrete system

axial stiffness and damping are linearly proportional to fluid viscosity (Booser 1984). Thus from Table 3, the axial stiffness and damping of spindle *A* are higher than those of spindle *B*. In the test, each HDB spindle motor carries a single disk with thickness of 1.27 mm. Figure 11 shows the test setup. The disk-spindle system is mounted on a very rigid fixture which is fixed on a shaker stand. During the test the motor spins at 7200 rpm and the shaker applies a random acceleration with a magnitude of 1 *g* rms along the vertical direction. The frequency of this random excitation ranges from 10 Hz to 1200 Hz. An accelerometer and a capacitance probe are used to measure the input acceleration and the axial vibration at outer radius of the top disk, respectively. A dynamic signal analyzer was used to determine the FRFs of the disk-spindle system based on the acceleration and vibration measured by the sensors.

Figures 12 and 13 compare the FRFs of the two tested spindles when they are stationary and spinning, respectively. In both figures, the resonance peak around 930 Hz is an unbalanced (0,0) mode. In the case when the motors are stationary, the vibration characteristics of both spindles are identical, as seen in Fig. 12. This shows that both spindles have the same design parameters except for the bearing lubricant properties. A comparison of Figs. 12 and 13 shows that the resonance amplitude reduces from 50 μm/g in the stationary case to ∼15 μm/g in the spinning case. The unbalanced (0,0) modes in the spinning case are heavily damped, because the fluid damping is activated and helps dissipate an energy from the system.

Figure 13 clearly shows that the HDB spindle with a higher viscosity or larger axial stiffness and damping has a higher amplitude of the unbalanced (0,0) mode. Compared with the HDB spindle with lower viscosity, the resonance

**Table 3.** Viscosity properties of the tested spindles

| Spindle type | Viscosity (mPas) |
|---|---|
| *A* | 34.2 |
| *B* | 10.5 |

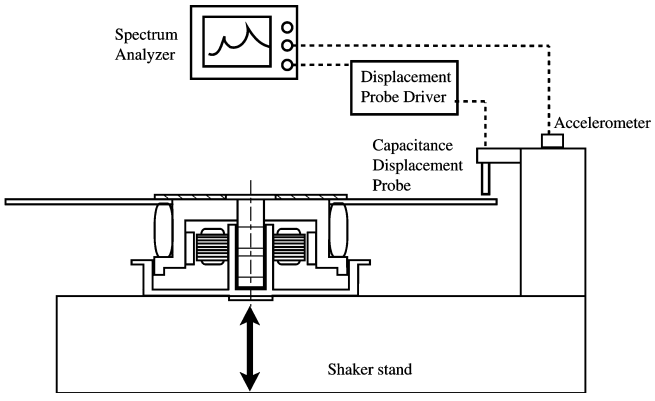


**Fig. 11.** Vibration test setup

amplitude of the spindle with higher viscosity is increased by 36%. This test result validates the prediction of the stiffness and damping effect on the axial vibration in Sect. 4. In conclusion, an increase in the axial stiffness and damping of the thrust bearing leads to a higher amplitude of the unbalanced (0,0) mode.

## 6 Conclusions

The parametric study reveals the following useful knowledge for the design of the thrust HDBs in disk drive spindles.

1. An increase in the axial stiffness and damping in thrust HDBs suppresses the axial vibration of the disk-spindle system at low frequency range. This is mainly because the larger stiffness significantly reduces the axial hub vibration which is the major component of the axial vibration in the low frequency range.
2. A too much increase in the axial stiffness and damping results in a higher amplitude of the unbalanced (0,0) mode. This is mainly because the higher damping results in the larger deflection of the disks which is the major component in the unbalanced (0,0) mode.

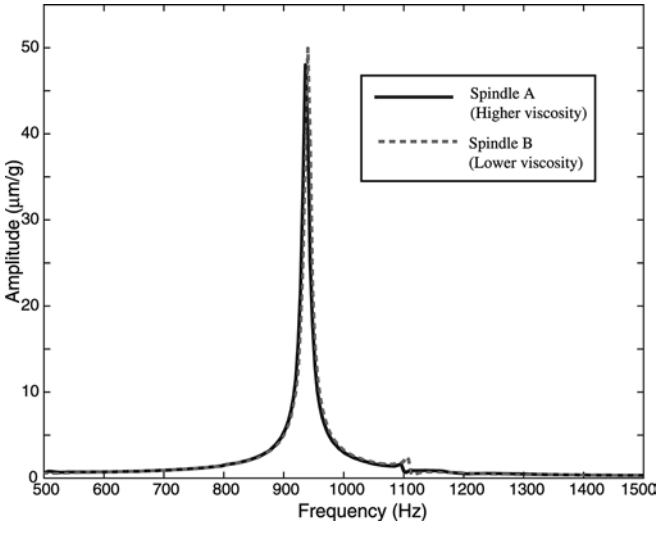


**Fig. 12.** Axial FRFs of a single disk HDB spindle systems at stationary

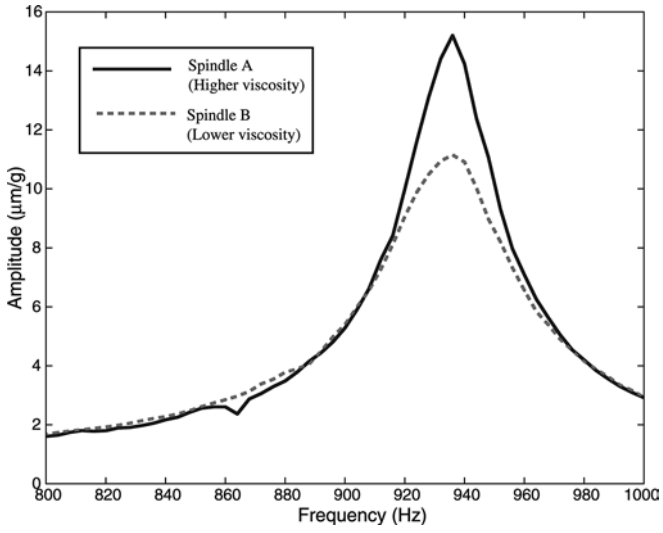


**Fig. 13.** Axial FRFs of a single disk HDB spindle systems at 7200 rpm

In practice, an optimal value of the axial stiffness and damping coefficients in thrust HDBs can be desired to minimize the amplitude of the unbalanced (0,0) mode.

## References

**Asada T; Saitou H; Asaida Y; Toujou K** (2001) Development of FDB spindle motors for HDD Use. IEEE Trans Mag 37: 783–788

**Booser ER** (1984) Handbook of Lubrication–Theory and Practice of Tribology. Vol II, CRC Press, Florida

**Jang G; Kim Y** (1999) Calculation of dynamic coefficients in hydrodynamic bearing considering five degree of freedom for a general rotor-bearing system. ASME J Tribol 121: 499–505

**Jintanawan T; Shen IY; Ku C-P** (1999) Free and forced vibration of a rotating disk pack and spindle motor system with hydrodynamic bearings. J Information Storage Processing Sys: 1: 45–48

**Jintanawan T; Shen IY; Tanaka K** (2001) Vibration analysis of fluid dynamic bearing spindles with rotating-shaft design. IEEE Trans Mag 37: 799–804

**Jintanawan T** (2002) FDB spindle motor design for vibration suppression. In Proc of APMRC 2002, pp 45–58

**Ku C-P** (1997) Effects of compliance of hydrodynamic thrust bearings in hard disk drives on disk Vibration. IEEE Trans Mag 33: 2641–2643

**Matsuoka K; Obata S; Kita H; Itoh F** (2001) Characteristic analysis of hydrodynamic bearings for HDDs. IEEE Trans Mag 37: 810–813

**Shen IY** (1997) Closed-form forced response of a damped, rotating, multiple disk/spindle system. J Appl Mech 64: 343–352

## Appendix

In Eqs. (3–6), $\eta$ and $b_0$ are inertia terms normalized with respect to the diametral mass moment of inertia of each disk $I_1$, given by

$$\eta = \frac{M}{I_1}, \quad b_0 = \frac{2\pi\rho h}{I_1}\int_a^b R_{00}(r)\mathrm{d}r \tag{26}$$

Furthermore $\omega_{00}$ is the natural frequencies of the axisymmetric disk mode, $\zeta$ is the normalized viscous damping of the disks as defined in Jintanawan et al. (2001), and $k_z$ and $c_z$ are total axial stiffness and damping of thrust HDBs normalized with respect to $I_1$:

$$k_z = \frac{1}{I_1}\sum_t k_{zz}^{(t)}, \quad c_z = \frac{1}{I_1}\sum_t c_{zz}^{(t)} \tag{27}$$

In (26) and (27) $M$ is the total mass of the disk-spindle system, $R_{00}(r)$ is the shape function of the axisymmetric disk mode, and $k_{zz}^{(t)}$ and $c_{zz}^{(t)}$ are axial stiffness and damping coefficients of thrust HDB, respectively. In addition, $a$ and $b$ in (26) are an inner radius and an outer radius of the disk.